University of Vermont Lake Carmi Monitoring 2020 Preliminary Report to the Vermont Department of Environmental Conservation Lakes and Ponds Program

Prepared by Andrew Schroth, Ashton Kirol, Mindy Morales-Williams, Kris Stepenuck

Key Findings:

● Aeration substantially decreased Lake Carmi's water column stability making it more susceptible to wind-driven mixing

● Aeration triggered substantial decreases in phosphorus internal loading in 2019 and 2020

● Aeration was unable to continuously maintain oxygen concentrations above the target nor fully suppress internal loading of phosphorus in either year, some of which was due to intermittent shutdowns of the system during crucial summer months

● Aeration appears to have altered the timing and composition of cyanobacteria blooms in Lake Carmi, however additional monitoring and analysis is required to confirm these impacts.

Introduction: 2020 was the second year of the aeration intervention, and here we present preliminary results from the first year of our research project. Where possible, we compare data from 2020 to pre-aeration (mostly 2018) and also to 2019 (the first year of aeration). Like 2019, intermittent multi-day malfunctions of the aeration system compromise our ability fully assess the capacity of the system to alter Lake Carmi's water quality and ecology. However, we have detected substantial changes to the lake's chemical and ecological system that have been facilitated by aeration that are discussed here. Our report first discusses weather and climate observations of 2020 for context. We then discuss how the aeration impacted the thermal and oxygen profiles of the lake and the impact of wind on fully mixing the system. We then discuss nutrient and metal time series collected by both UVM and VT DEC, focusing on the extent to which geochemical signatures of internal loading were detected in 2020, and how that compares to historical time series collected by VT DEC. Our final section discusses processed biological time series from both sensors (2020) and integrated water samples (2018 and 2019). In all cases, analysis should be considered preliminary, and substantial additional analysis will occur over the remaining 1.5 years of the project. This report is designed to provide VT DEC practitioners our synopsis of what we have observed thus far and tentative inferences that can be drawn.

2020 Weather and Climate: While early spring 2020 was slightly wetter than average, in the beginning of May, the accumulated precipitation for the year fell behind average and the rest of the year was drier than average in total accumulation. August 2020 was relatively wet, but nearly

half of the monthly precipitation occurred in one day early in the month. September was much drier than 2018 or 2019, and most of the precipitation occurred over the last two days of the month. The nearly two-month period between the large August and September storms was very dry. Air temperatures in the summer months were slightly warmer than 2019 and generally fluctuated between above and within the average summer temperature range. In general, these data demonstrate that the summer could be classified as relatively hot and dry compared to a typical summer in the region.

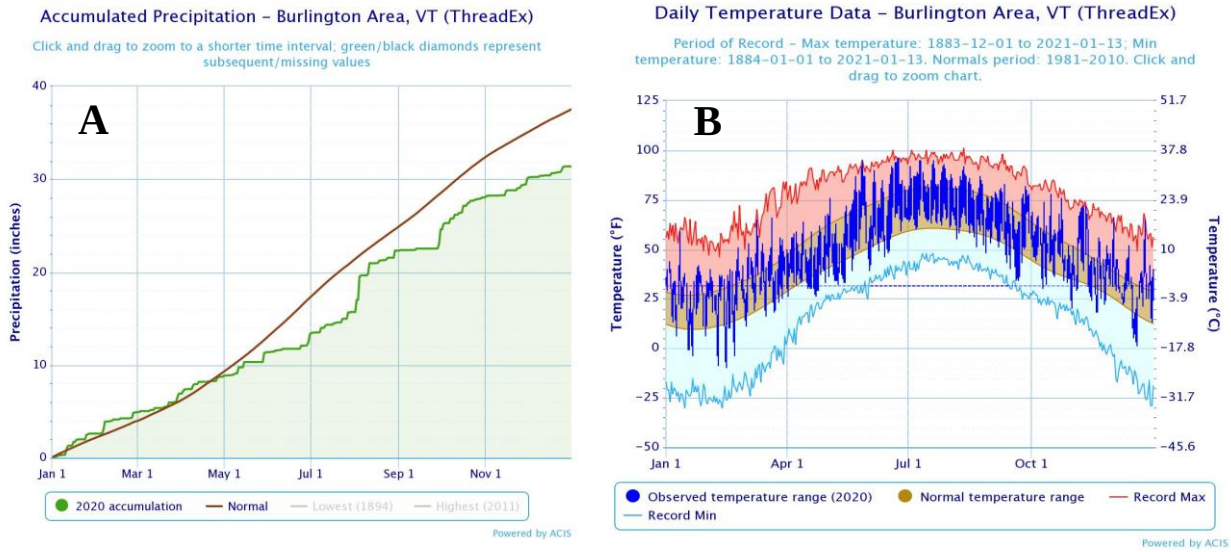

Figure 1: Historical cumulative precipitation amounts and daily temperature ranges and 2020 data for Burlington, Vermont.

2020 Thermal Stratification: Here we examine the impacts of aeration on water temperature and dissolved oxygen based on data from our sensor chains spanning 2018 through 2020 where the impacts of aeration are pronounced. In both 2019 and 2020, thermal stratification was allowed to set-up in June prior to turning the aeration system on, more so in 2019 relative to 2020 (Figure 2). Consequently, there was a time lag between turning the system on and breaking down water column stability and fully mixing the water column in both years. In 2020, aeration was initiated on an earlier date at a cooler temperature under less stratification, and a large wind event shortly thereafter allowed the system to mix more rapidly than in 2019 when the system was instead turned on under summer stratification conditions during a period of sustained hot and calm weather. However, during a subsequent time period where the system was not fully

functional, thermal stratification quickly redeveloped under hot, low wind conditions in 2020. It is also important to note that, in both 2019 and 2020. Once the aeration system was turned on, bottom water tended to be warmer relative to the reference condition in 2018, and? peak summer surface water temperatures tended to be slightly lower due to sustained mixing relative to the reference system. These warmer summer bottom waters have the capacity to enhance sediment oxygen demand both through decreased oxygen saturation, redox gradients, and increased microbial activity at elevated temperatures. Such demand will promote the resilience of low sediment-water interface (SWI) oxygen conditions as the aeration system works to break down water column stability. This will be subsequently discussed.

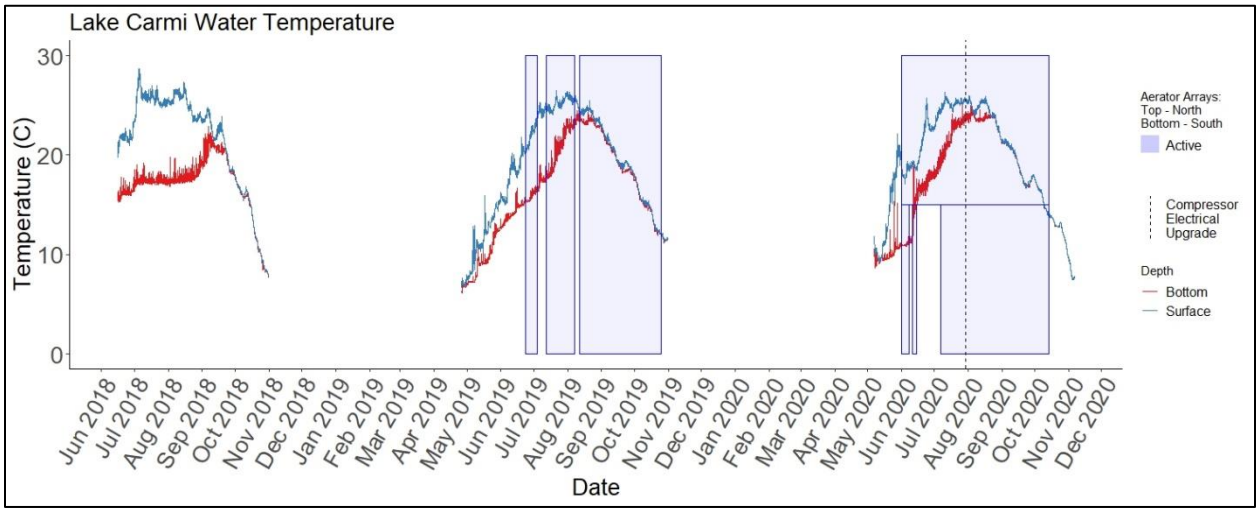

Figure 2: Lake Carmi water temperature 2018-2020. Blue is surface reading (~0.5 meters), Red is bottom reading (near the sediment-water interface). Shaded panels are when the aerator was fully operational, whereas breaks in the blue shading is indicative of one or both arrays being compromised. A full break means that both (northern and southern) arrays were shut down, while a partial break is indicative of only one of the arrays being down.

The water column stability (Schmidt stability) calculated from the thermal profile of the water column and the lake bathymetry is an estimate of the energy needed to mix the entire lake to a uniform temperature. Indeed, this is a useful metric to assess how the aeration system has changed the lake by comparing stability between 2018 and 2020. Both 2018 and 2020 had a similar maximum stability value near 85 J/m^2 (Figure 3). In 2020, this maximum value was reached before the aerator was turned on. The aeration system in 2020 was able to break down most of the thermal stratification over time, which lowers the energy required to mix the water column as seen in the time series below (large difference between the red and blue lines during

summer). The average water column stability was nearly three times higher in 2018 without the aeration system (2018: 33 J/m^2, 2020: 11 J/m^2). Periods of very low wind can still lead to low bottom dissolved oxygen, but much lower windspeeds were needed in 2020 to mix the lake throughout the period where the aeration system was functioning. The changing water column stability and associated threshold of wind mixing and its relation to the aeration is also evident from the three-panel plot below. There was a decrease in stability over time as aerator functionality improved over the course of summer, and lower wind speeds were required for stability to approach zero late in the summer relative to early in the summer (e.g. a wind speed that would fully mix the system in the lake in late August would not achieve this in early July).

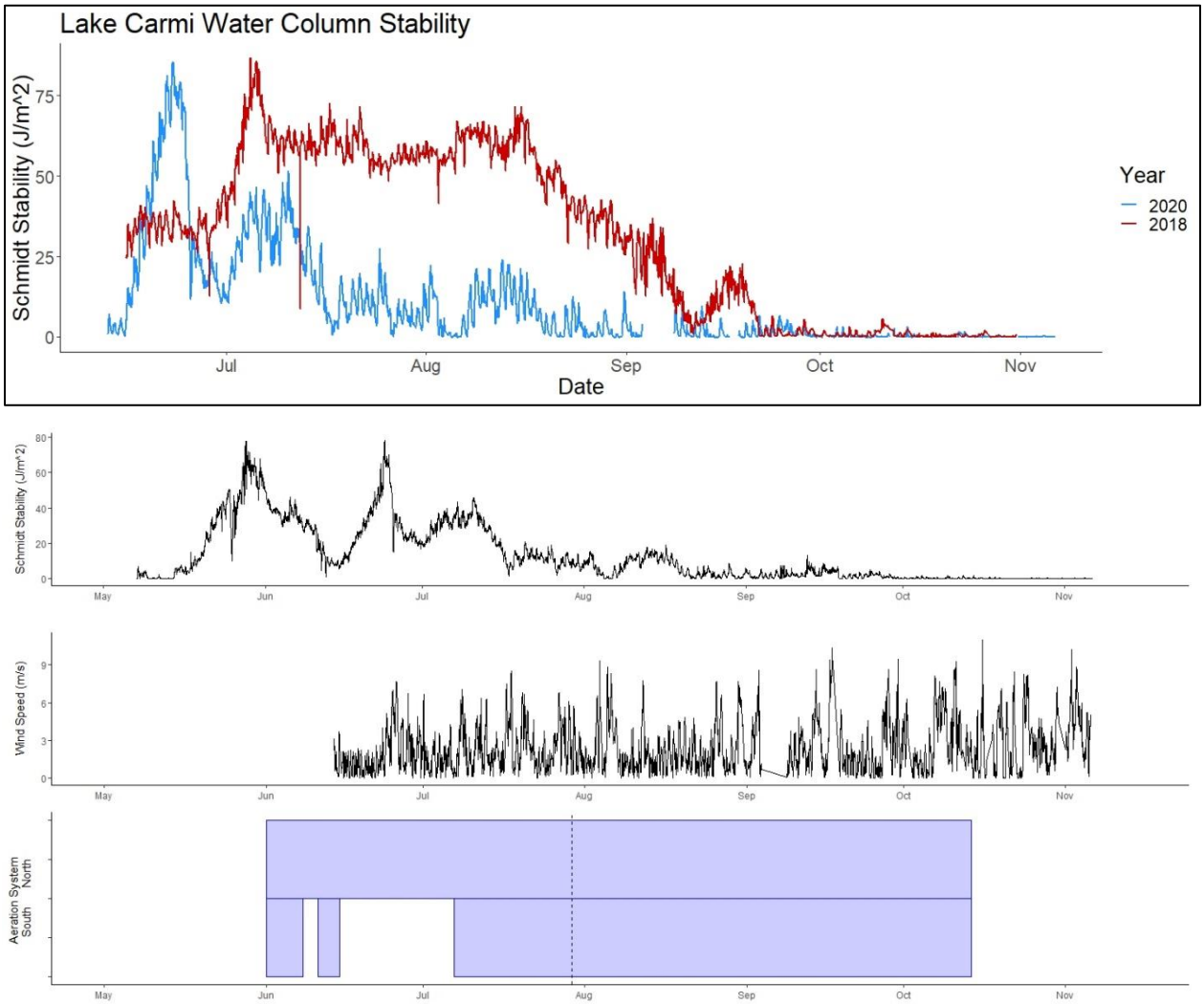

Figure 3: A Schmidt stability of Lake Carmi's water column in 2018 (red pre-aeration) and 2020 (blue, under aeration). **B** 2020 Schmidt stability with concurrent wind measurements and aeration operations. This illustrates how the aerator makes the system much less stable and more prone to wind mixing when functioning. These data also illustrate how quickly water column

stability can recover when the aeration system is compromised, and winds are low (e.g. late June of 2020).

2020 Dissolved Oxygen Dynamics: While the impacts of the aerator on lake physics are obvious and in-line with predictions, the impacts on dissolved oxygen in 2020 are more complex. The southern (park) aeration system shutdown on 6/15 coincided with a period of warm air temperatures and low wind(Figure 2 and 3). This caused dissolved oxygen (DO) to decrease relatively rapidly over the course of a few days to well below the 2.5 mg/L threshold (Figure 4). Thermal stratification developed, making the water column more stable and resistant to wind mixing. For example, cooling air temperatures and high winds (up to 13 m/s gusts) between 6/24 and 6/25 caused a decrease in surface water temperatures and water column stability, but there was no consequent increase in bottom water dissolved oxygen because sufficient thermal stratification remained. The southern (park) aeration system was repaired on 7/7. While that too triggered decreased water column stability, sediment oxygen demand was high enough to sustain low oxygen conditions near the SWI. At this point, the bottom water dissolved oxygen recorded by the profiler was consistently below 2.5 mg/L. Several wind events (> 4m/s) over the next week were unable to mix the bottom water and dissolved oxygen remained low. There was a decrease in surface temperature and a continued increase in bottom temperature once the aeration system was repaired that resulted in further decreased water column stability. Increased wind on 7/17 and 7/18 (5 to 8 m/s) led to mixing that broke down stratification temporarily (< 1^{o} C temperature difference, < 1 mg/L DO difference). Dissolved oxygen profiles were extremely dynamic during periods when the water was warm, cyanobacteria were active, and stability was low due to aeration. For example, between 7/16 and 8/03 there were fluctuating periods of low bottom dissolved oxygen and mixing driven largely by wind, but also likely impacted by the balance between phytoplankton primary production via photosynthesis (oxygen generation) and phytoplankton and heterotrophic respiration (oxygen uptake). Indeed, diurnal surface water DO signals coupled with saturated to supersaturated warm surface water DO profiles are characteristics of waters where photosynthesis associated with a bloom impacting oxygen profiles. In some cases, bottom water dissolved oxygen dropped from over 8 mg/L to under 2 mg/L and rose back to 8 mg/L in a course of 12 hours as wind shifted. Frequent high winds (>6 m/s) between 8/03 and 8/06 mixed the water column, and high bottom DO was sustained even when low winds persisted for several hours during this time. However, a more sustained period

of low wind between 8/06 and 8/19 again led to the return of periods of low bottom water dissolved oxygen. Mixing occurred on 8/20 following sustained winds (> 4 m/s). Temperature stratification was minimal for the remainder of the season, and low wind thresholds were required to increase bottom DO. In this period, it appears that 3 m/s winds were capable of mixing the water column, and 1-2 m/s winds were capable of maintaining high well-mixed DO profiles. Bottom DO concentrations remained high (> 6 mg/L) for the remainder of the monitoring season despite periods of very little wind as is often typical in fall-note the similarity between water column stability and DO concentrations in October and November of 2018 and 2020.

The take home point from this time series is that while the system when functioning at capacity does a good job of breaking down water column stability, it also sets up highly dynamic conditions where warm bottom waters can plunge to below the threshold dissolved oxygen concentrations if the lake is under low wind, and high air and bottom water temperature conditions. It is not evident from either the 2020 or 2019 time series that the fully operational system can maintain an oxidized sediment water interface under sustained hot temperature and low wind conditions. Stratification of little more than a degree C is enough to drive bottom water to a low oxygen state at or below the target of 2.5mg/L (Figures 2 and 4). It is not clear at this time to our research team whether or not a full season of full aerator functionality would change that, which makes it challenging to assess performance based on years with large operational disruptions occurring in summer.

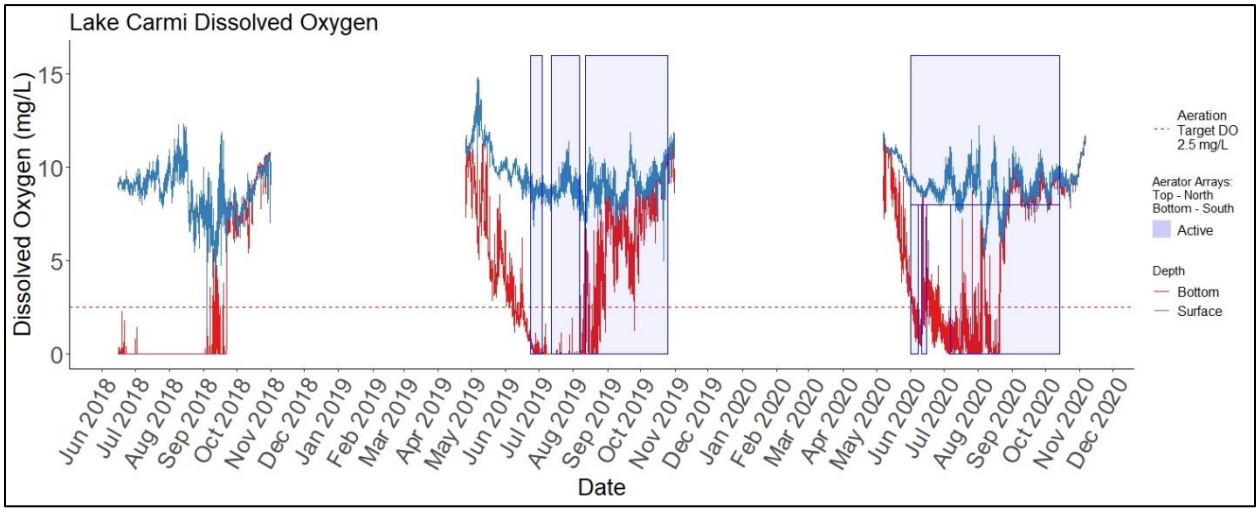

Figure 4: Water column dissolved oxygen high frequency time series from 2018-2020 fixed buoys. Red line is bottom water (~9 meters) and blue line is surface water (~0.5 meters), The red dotted line is the 2.5 mg/L target.

It is also informative to compare the bottom water dissolved oxygen measured by our fixed thermistor/DO chain relative to that of our profiling system (Figure 5), as the fixed position of the former allows us to measure DO at the SWI (sensor placed immediately above the anchor) while the profiler comes within ~ 0.5 meters of the bottom. As expected, dissolved oxygen concentrations were significantly lower in the deeper sensor and frequently anoxic. Such steep redox gradients are consistent with the literature around SWI geochemistry. These data are likely more reflective of the conditions that the sediment is exposed to, and in subsequent nutrient data, it is evident that those anoxic conditions triggered P release from sediment inventories, albeit at much lower levels than previous years.

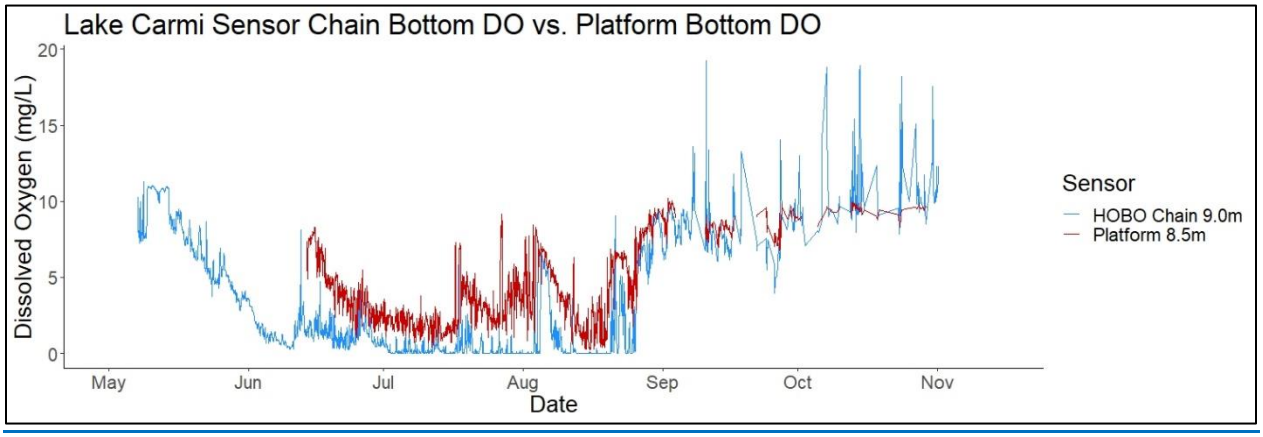

Figure 5: Comparison between profiler bottom measurement at 8.5 meters (blue line) and HOBO chain measurement at 9 meters (red line). This illustrates the sharp DO gradients typical of the sediment-water interface and that DO concentrations were at or near zero for much of the summer of 2020.

Internal P Loading in 2020: It is evident from the 2020 time series that while internal loading was substantially suppressed relative to pre-aeration time series (where DEC detected strong P stratification due to sustained anoxic conditions at the SWI), there were still periods of low oxygen conditions that promoted internal loading of phosphorus (P). Internal loading events were detected in the UVM time series (P stratification/bottom water P enrichment is not detected in the 2020 DEC time series), where sample intakes were 0.5 meters closer to the SWI than VT DEC's deepest sampling point (Figure 6). Indeed, the highest concentrations of bottom water P were measured on the days where bottom water sensors detected an anoxic SWI when the aeration system was compromised. When subsequent mixing occurred when the fully functional

aeration system was restored and wind fully mixed the water column, full water column enrichment in P also occurred. That is evident in the DEC time series roughly doubling the concentration of P in the water column. Water column-wide P concentrations became slightly more enriched after another anoxic SWI excursion followed by mixing. Interestingly, a similar trend was observed in 2019 in the DEC time series where internal loading occurred during a more sustained period of an anoxic SWI (in this case the SWI went fully anoxic prior to the system being turned on), and the more sustained anoxia allowed for the DEC to detect the process at their 8 meter depth sampling point. Similarly, in 2019, subsequent mixing, driven by the aeration system breaking down water column stability, facilitated the entire water column becoming enriched in P. Indeed, the mixed water column TP concentrations in 2019 and 2020 following periods of internal loading are quite comparable in temporal structure and concentrations. In both years, summer and fall TP concentrations in the mixed water column were over double the TMDL target for Lake Carmi. This similar trajectory of each aeration year is interesting given their large differences in weather between the two summers (relatively wet in 2019, relatively dry in 2020). In both cases, summer and early fall spikes in water column P correspond to spikes in Mn, which is redox sensitive transition metal that is a common indicator of redox-driven P release. Interestingly, aerator mixed water column P concentrations also appear comparable to the post fall turnover concentrations detected in the pre-aeration component of the time series as monitored by DEC. In an ideal scenario, the aeration system would be turned on prior to the bottom water going anoxic and well-mixed summer water column concentrations would remain comparable to those of late spring/early summer around the TMDL target. However, based on these data, it is unclear at this time if the aerator can fully keep the sediment from going anoxic and suppressing internal loading given the system shutdowns that have occurred that allowed for internal loading to occur, and subsequent mixing facilitated enrichment of the entire water column to concentrations well above the target.

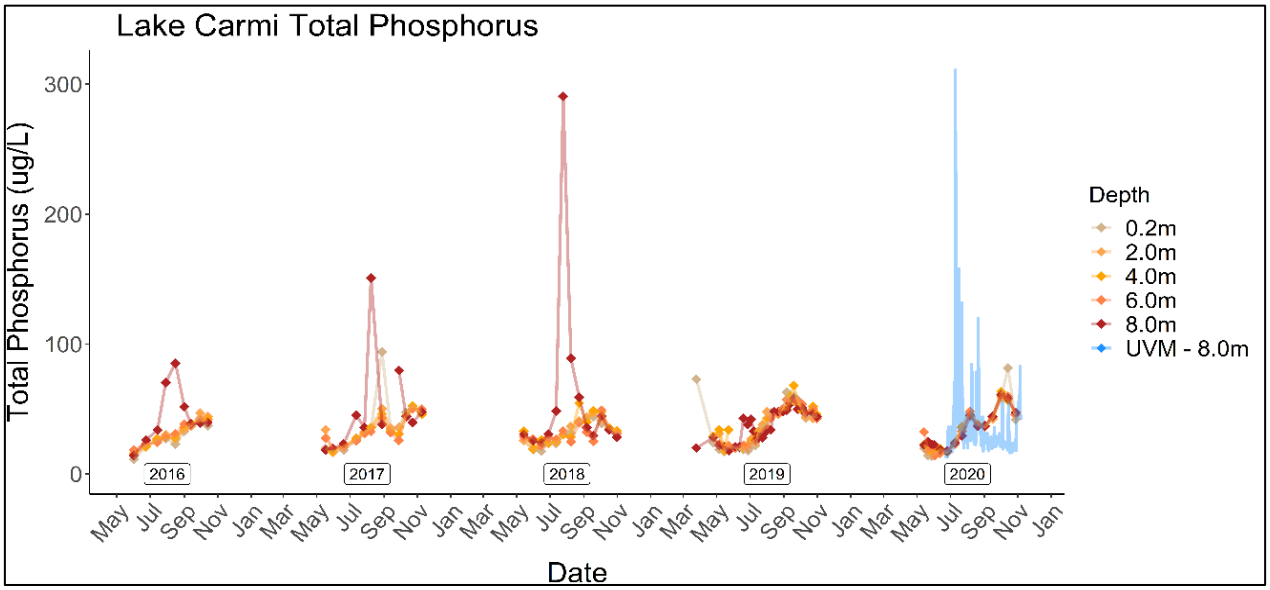

Figure 6: VT DEC and UVM total phosphorus time series-2016-2020. High values in red in 2016-19 and blue in 2020 relative to shades of orange indicate periods of internal loading. Blue lines are bottom water daily samples collected by ISCO with an intake positioned at ~8.5 meters. Internal loading is evident in the 2020 time series that was not detected by the VT DEC monitoring program until the water column mixed.

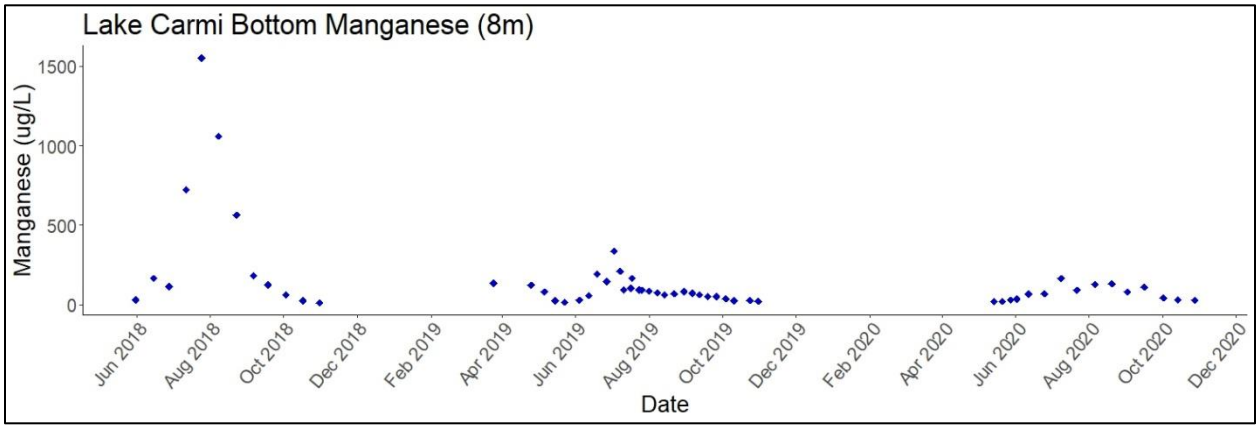

Figure 7: VT DEC bottom water manganese concentrations. Spikes in bottom water manganese often coincide with periods of redox driven internal release of P.

Sediment Time Series: Redox sensitive phosphorus (the pool of phosphorus in sediment that is likely to be released under low DO) in the top ten centimeters of lake sediment was relatively stable in 2020 and most of the variability was within 10 % of the concentration. For context, when we collected two sediment cores in 2018, one under summer anoxic conditions and one post fall turnover, there was a ~50% difference in the concentration of redox sensitive P in the upper two centimeters during those two time points (a relatively high sediment P concentration in fall after mixing, a relatively low sediment P concentration in midsummer during 2018

sustained anoxia). This suggests that there was much more extensive release and re-accumulation of phosphorus in the natural, more dimictic system, perhaps indicating that aeration has partially suppressed internal loading of P. This is also supported by the particularly high bottom water TP concentrations detected in the DEC dataset under sustained stratification (e.g. high concentrations at 8 meters building over the course of the summer of 2018) that were less evident in 2019 and not evident in 2020 DEC water monitoring. Under aeration, there was less internal loading detected in the water, and those lower fluxes likely promoted a more consistent concentration of P in the sediment. In the surface sediments that are typically most reflective of sediment-water interactions and transfers between these pools, we did see some decrease in P during the initial June stratification event that corresponded to increase in the water column (Figure 6), and some subsequent re-accumulation as the system became mixed by the aerator and windy conditions. The decrease in late fall under sustained oxic conditions is most likely a result of forming more stable P phases that were not released by this relatively weak extractant (ascorbate) rather than any sort of internal loading event.

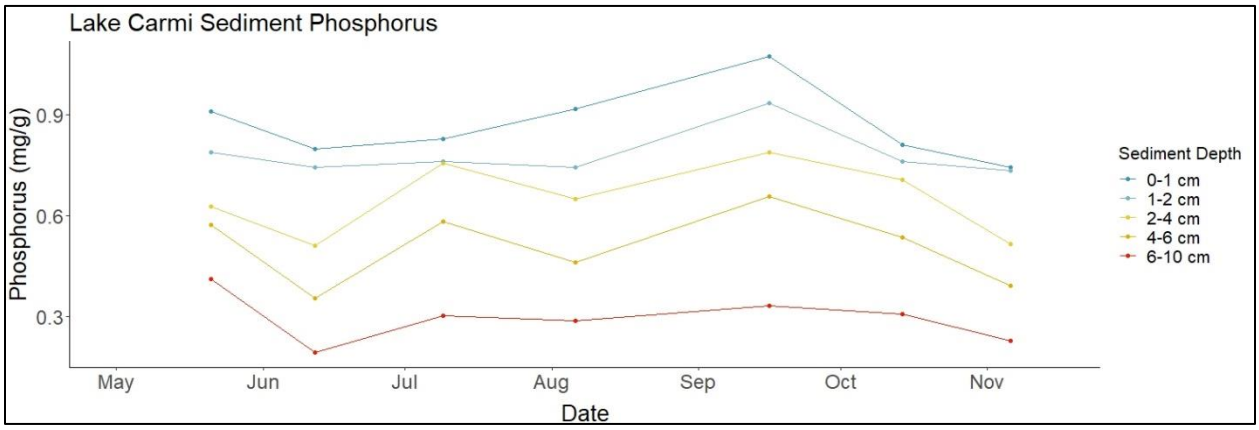

Figure 8: Lake Carmi sediment core concentrations of redox sensitive phosphorus in 2020 at different depth intervals.

Biological Data: Thus far, neither the data from 2019 nor 2020 suggests that the aeration system has been able to suppress the occurrence of cyanobacteria blooms in the lake, which is not surprising given the observed concentrations of P under aeration. Preliminary analysis does indicate that the aeration system has affected the timing and composition of the blooms. It is somewhat challenging to directly link such changes to aeration, given that bloom dynamics are also heavily impacted by natural variability in weather/climate, coupled with the uncertainty surrounding inconsistent aerator performance of the monitoring years. That being said, our initial

analysis suggests some fundamental impacts of the aerator on bloom dynamics that will be discussed here.

In both monitoring years of aeration, the bloom initiated following aeration-induced mixing of previously anoxic bottom water under warm surface water conditions (~25 degrees C). This is not surprising, as in the years preceding installation, the strongest blooms tended to occur when there was a natural mixing event (e.g. fall turnover), followed by sustained warm conditions (e.g. 2017). Having those mixing events in early summer provides those internal loads to the entire water column at the time when the water column is just warming into temperature ranges preferred by cyanobacteria. Thus, the aerator can serve as a nutrient source if it is intermittently compromised (or turned on too late in spring) allowing the SWI to go anoxic, and subsequent repair can provide a mixing-derived pulse of bottom water nutrients to a warm water column and trigger a bloom earlier than would otherwise occur. In addition, disruption of sediments can recirculate or trigger growth of cyanobacteria resting cells, which then migrate to the upper water column.

In general, in 2020 there was sustained bloom activity from July into October at various levels. The first noticeable rise in phycocyanin occurred on 7/18 after two days of mixing that followed prolonged low bottom DO conditions and consequent internal P loading. Phycocyanin levels continued to rise until 7/31, which was the maximum reading observed in the entire time series. Phycocyanin relative fluorescence dropped suddenly as the lake mixed in early August, then rose as the lake re-stratified in mid-August. Phycocyanin dropped again with the mixing of the lake around 8/20 and remained lower for the remainder of the season when the lake was relatively well-mixed, but at a higher level than pre-bloom. However, there were reports of blooms after the drop in phycocyanin reading detected by the platform sensor that were visually detected by local residents. However, there was not strong visual evidence of blooms at the platform during those late August collection days, supporting the interpretation that these later blooms were mostly focused on the shoreline. Additionally, the changing ratio of the different biological pigments over time (higher phycocyanin relative to chlorophyll-A fluorescence and vice versa during different bloom periods) could be reflective of shifting bloom compositions over time. In progress analysis of the community composition of 2020 blooms will allow us to assess if and

how the cyanobacteria phytoplankton community in 2020 may have differed from 2018 and 2019, as well as how it developed over the course of the summer and fall.

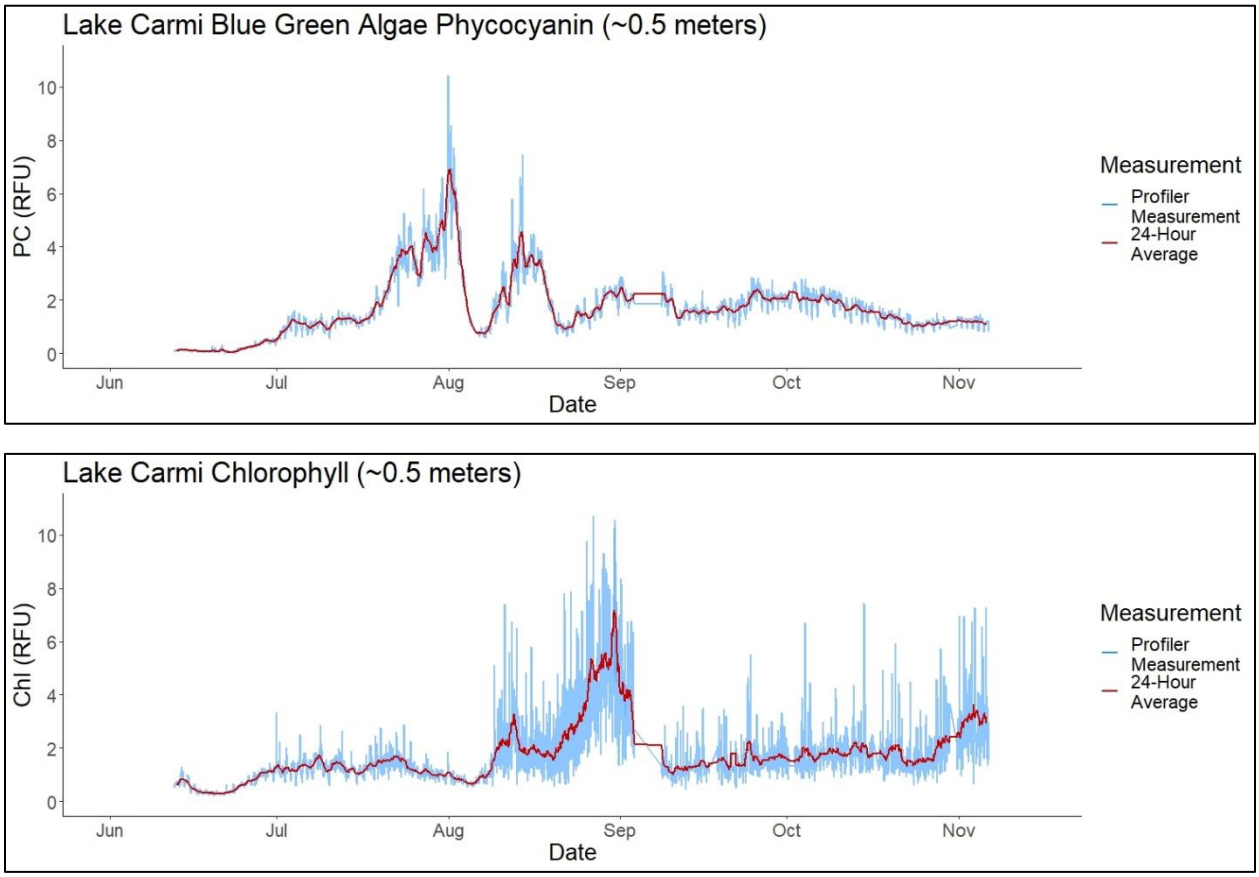

Figure 9: Relative fluorescence of the biological pigments phycocyanin (PC upper figure) and chlorophyll (Chl lower figure). Note, while increases in phycocyanin suggest increasing abundance of cyanobacteria in the location of the sensor, this is not a quantitative estimate.

We can also report additional new biological analysis of samples collected during 2019. While we do not have overlapping high frequency sensor data to inform 2019 data, grab samples were collected by Pete Stengel for analysis of the phytoplankton composition and abundance in Dr. Mindy Morales-Williams' lab. A similar dataset exits for the pre-aeration year of 2018. Although we cannot directly attribute the differences between 2018 and 2019 phytoplankton communities to aeration, there were interesting differences that could be related to the aeration intervention. The timing of bloom initiation was substantially earlier in 2019 and seemingly triggered by the aerator mixing a previously stratified water column (a similar response is evident in the 2020 data based on the phycocyanin time series). The bloom was also more diverse and dynamic in its composition in 2019 relative to 2018, and increasingly dominated by N-fixing filamentous

cyanobacteria taxa which have a dormant resting stage in sediments and may be triggered to emerge if the sediment-water interface is disrupted by aeration. There was slightly less phytoplankton and cyanobacteria biomass in 2018 relative to 2019, but that difference was within observed variability and not statistically significant.

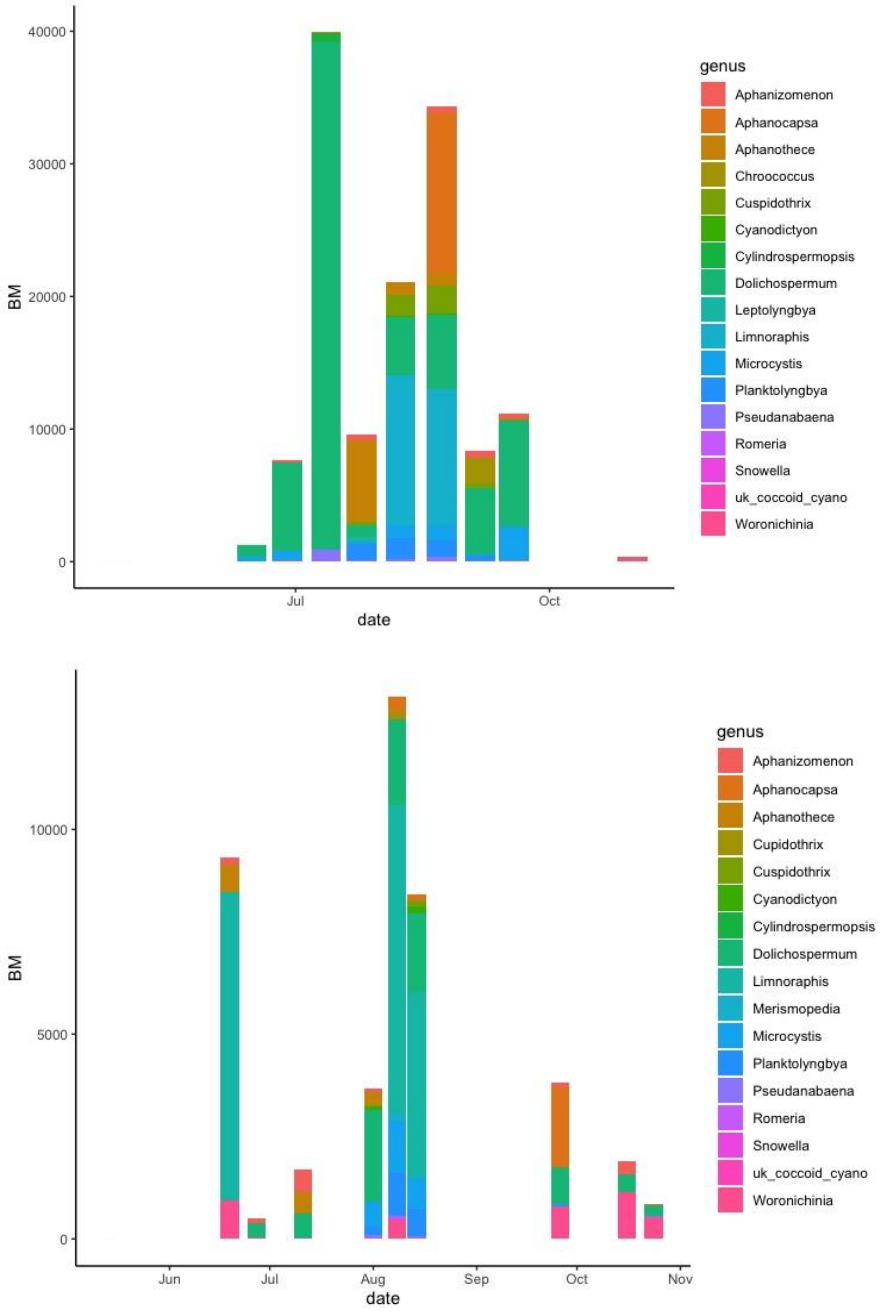

Figure 10: Cyanobacteria community biomass in 2018 and 2019

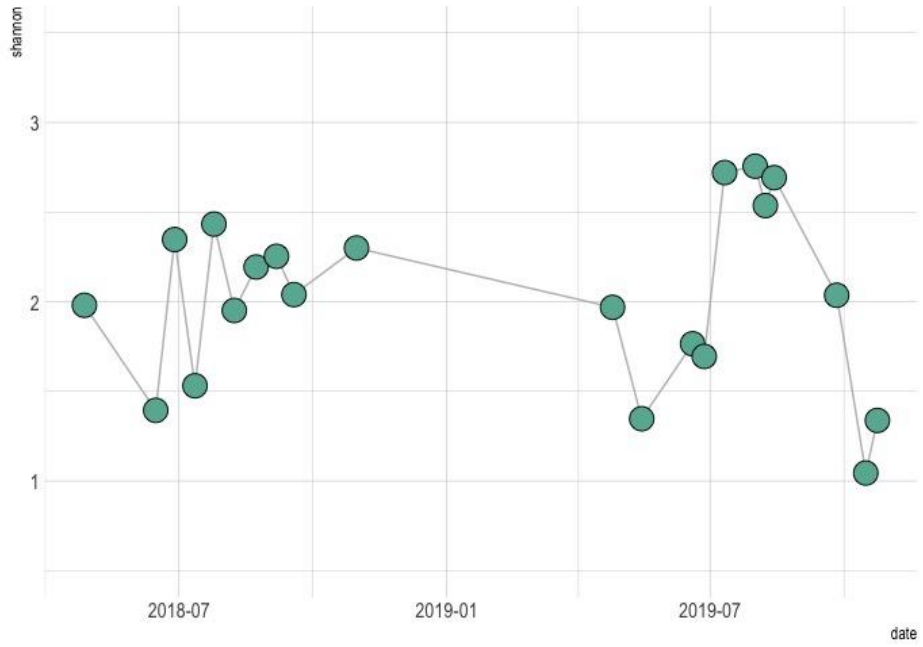

Figure 11: Shannon diversity index of cyanobacteria species. Higher numbers equate to more species diversity. The most diverse samples were collected following the initial aeration in 2019.